ELSEVIER

Biophysical Chemistry 125 (2007) 549–555

Biophysical Chemistry

http://www.elsevier.com/locate/biophyschem

Temperature dependence of binding and catalysis for the Cdc25B phosphatase

Jungsan Sohn [1], Johannes Rudolph *

Department of Biochemistry and Chemistry, Duke University Medical Center, Durham, NC 27710, USA

Received 6 November 2006; received in revised form 21 November 2006; accepted 21 November 2006
Available online 29 November 2006

Abstract

Using a combination of steady-state and single-turnover kinetics, we probe the temperature dependence of substrate association and chemistry for the reaction of Cdc25B phosphatase with its Cdk2–pTpY/CycA protein substrate. The transition state for substrate association is dominated by an enthalpic barrier ($\Delta H^{\ddagger}$ of 13 kcal/mol) and has a favorable entropic contribution of 4 kcal/mol at 298 K. Phosphate transfer from Cdk2–pTpY/CycA to enzyme ($\Delta H^{\ddagger}$ of 12 kcal/mol) is enthalpically more favorable than for the small molecule substrate *p*-nitrophenyl phosphate ($\Delta H^{\ddagger}$ of 18 kcal/mol), yet entropically less favorable ($T\Delta S^{\ddagger}$ of 2 vs. −6 kcal/mol at 298 K, respectively). By measuring the temperature dependence of binding and catalysis for several hotspot mutants involved in binding of protein substrate, we determine the enthalpy–entropy compensations for changes in rates of association and phosphate transfer compared to the wild type system. We conclude that the transition state for enzyme–substrate association involves tight and specific contacts at the remote docking site and that phospho-transfer from Cdk2–pTpY/CycA to the pre-organized active site of the enzyme is accompanied by unfavorable entropic rearrangements that promote rapid product dissociation.

Keywords: Protein–protein interactions; Protein tyrosine phosphatase; Single-turnover kinetics; Thermodynamics

1. Introduction

Understanding the mechanisms by which enzymes achieve tremendous rate enhancements is one of the main goals of protein biochemistry. Other than scrutinizing the chemistry of the reaction at the active site, it is important to understand how enzymes specifically recognize their substrates. For the myriad of different regulatory enzymes that utilize protein substrates, specific substrate recognition is a particularly complex and critical part of catalysis. To avoid possible crosstalk arising from highly similar sites of chemistry, protein kinases and phosphatases have developed sophisticated mechanisms for binding their physiological substrates. These enzymes often utilize docking sites located remote from their active sites. Docking sites ensure accurate recruitment of protein substrates and can lead to significant enhancement of catalytic efficiency. Interestingly, although protein docking sites typically encompass extensive protein–protein interfaces, only 5–10% of the residues at these interfaces, so-called hotspot residues, contribute significantly to the energetics of binding, with the remaining majority apparently serving as tolerant bystanders [1,2]. The role of thermodynamics for hotspot residues in protein substrate recognition has been dissected for only a few protein–protein complexes including RNases with their protein inhibitors [3], Ras with its effector proteins Raf and RalGDS [4] and antibodies binding to lysozyme [5,6]. Herein we investigate the temperature dependence of substrate recognition and subsequent catalysis for Cdc25B phosphatase and its protein substrate, the bis-phosphorylated cyclin-dependent kinase 2 complexed with Cyclin A (Cdk2–pTpY/CycA). Cdc25B phosphatase regulates the eukaryotic cell cycle by activating the Cdk/cyclin complexes. For this enzyme–substrate pair, the docking site >20 Å from the active site is energetically defined by the interactions between three hotspot residues on Cdc25B (Arg488, Arg492, and Tyr497) and one hotspot residue on Cdk2

Abbreviations: Cdk2–pTpY/CycA, cyclin-dependent kinase 2 complexed with cyclin A and bis-phosphorylated on Thr14 and Tyr15; PTP, protein tyrosine phosphatase; pNPP, *p*-nitrophenyl phosphate; E.S, enzyme–substrate.

* Corresponding author. Tel.: +1 919 668 6188; fax: +1 919 613 8642.
E-mail address: rudolph@biochem.duke.edu (J. Rudolph).
[1] Current address: Department of Biology, MIT Cambridge, MA 02139, USA.

0301-4622/$ - see front matter © 2006 Elsevier B.V. All rights reserved.
doi:10.1016/j.bpc.2006.11.005

(Asp206) (Fig. 1) [7,8]. Mutations of these hotspot residues on either the enzyme or the substrate decrease activity (k_{cat}/K_m) by reducing the rate constant for association (20- to 900-fold) [9]. In addition, the C-terminal tail of Cdc25B serves as an independent albeit less significant (10-fold) element in the recognition of protein substrate [7,10]. We build on these prior detailed enzymological investigations by applying transition state theory to dissect the enthalpy–entropy contributions in the process of substrate association. Also, in comparison to the small molecule substrate *p*-nitrophenyl phosphate (pNPP), we probe the temperature dependence of the kinetics of phosphate transfer from substrate to form the phospho-enzyme intermediate.

2. Materials and methods

2.1. Protein expression and purification

The catalytic domain of Cdc25B and its R488L, R492L, and Y497A mutants were expressed as untagged proteins in *Escherichia coli* as described [11,12]. The Cdk2/CycA complex and the D206A mutant of Cdk2, in which CycA is truncated and encompasses residues 174–432, was prepared as previously described [13,7]. The soluble domain of the dual-specificity kinase Myt1 was expressed as a GST-tagged protein in *E. coli* [14] and purified as described [15]. The bis-phosphorylated Cdk2–pTpY/CycA substrate was prepared by incubation of Cdk2/CycA with GST-Myt1 bound to glutathione–Sepharose beads and 2.5 mM [γ-^{32}P]-ATP (200–500 Ci/mol) for 2.5 h at room temperature. Remaining ATP and GST-Myt1 were removed by G-50 chromatography.

2.2. Steady-state and transient kinetics

All phosphatase reactions were performed in a three-component buffer (50 mM Tris, 50 mM Bis–Tris, 100 mM Na acetate, pH 6.0–6.5) containing 2 mM dithiothreitol. Activity of Cdc25B with Cdk2–pTpY/CycA was assayed by monitoring release of inorganic phosphate from pThr14. Reactions were initiated by enzyme in the presence of 1 mg/ml BSA and 0.05% Tween 20, and quenched and precipitated by adding 3–5 volumes of 30% trichloroacetic acid (TCA). After centrifugation at 4 °C at 14 000×*g* for 20 min to remove unreacted substrate, the supernatant was subjected to scintillation counting. For k_{cat}/K_m measurements, time dependence (5 points minimum), substrate concentration dependence (2–3 differing concentrations between 50 and 160 nM), and enzyme concentration dependence (3–4 differing concentrations, see below) were tested to ensure adherence to Michaelis–Menten conditions. For assays with wild type substrate, enzyme concentrations were 0.8–3 nM for wild type Cdc25B, 0.1–3 μM for R488L, R492L, and Y497A, and 7–20 nM for the mutant of Cdc25B lacking the C-terminal tail. For assays with the D206A mutant of the substrate, 0.2–1 μM wild type Cdc25B was used. All single-turnover assays were performed using at minimum a 5-fold excess of the enzyme Cdc25B over the substrate Cdk2–pTpY/CycA. Single-turnover experiments on the time scale of 5 s to 10 min were performed using manual quench as for the steady-state experiments. Single-turnover experiments on the time-scale of 10 ms to 3 s were performed using rapid quench flow (RQF-400, Bio-Logic). Reactions were initially quenched with 2 M HCl. An equal volume of 30% TCA was subsequently

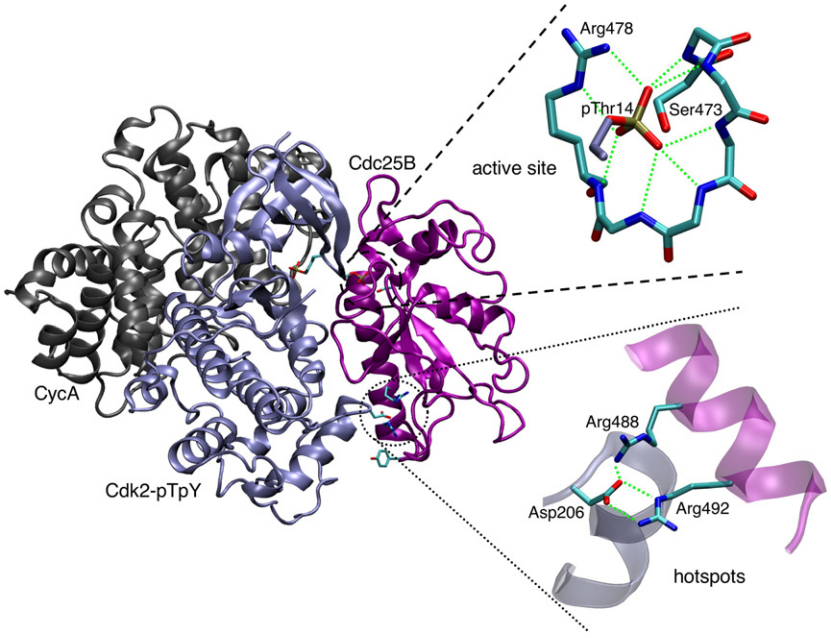

Fig. 1. Docking model of Cdc25B with its substrate Cdk2-pTpY/CycA highlighting the interactions at the active site of Cdc25B and at the remote docking site. The substrate-trapping mutant of Cdc25B(C473S), bis-phosphorylated Cdk2, and CycA are shown in cartoon representation in purple, blue, and gray, respectively. A dashed circle denotes the active site region, with the detail showing how the backbone amides of the active site loop along with Arg478 of Cdc25B cradle the pThr14 of the protein substrate. A dotted circle denotes the hotspot region, with the detail showing the ionic hydrogen bond interactions that govern association of protein substrate.

added to precipitate the proteins, and released phosphate was quantitated as described for the steady-state measurements. At least two different substrate concentrations (50–150 nM) and four different enzyme concentrations (6–16 μM) were used to verify adherence to single-turnover conditions. The stability of enzyme at varying temperatures was tested using the small-molecule substrate pNPP (see below). The stability of protein substrate at varying temperatures was tested by quantitating total product formation, with extended incubation at temperatures >30 °C showing significant reduction (20–30%), and limiting our temperature-dependent analysis to 5–25 °C. Insufficient mixing in the rapid quench due to increased viscosity at temperatures <10 °C limited the temperature-dependent measurements of k_2 for the wild type enzyme to 13–25 °C. The stability of the pH (6.3–6.5) in the reaction solutions was confirmed over the range of temperatures. Assays with the small molecule substrate *p*-nitrophenyl phosphate (pNPP) were performed by UV–VIS spectroscopy in a Hewlett-Packard diode array spectrophotometer at 410 nm ($\varepsilon = 5142\ M^{-1}\ cm^{-1}$, at pH 6.5) in 8×1 mL cuvettes and a thermostatted (7–25 °C) multi-cell holder. The values for k_{cat} and K_m were determined using eight different concentrations of substrate between 0.2 and 5× K_m and an enzyme concentration of 0.2 μM.

2.3. Data fitting

We rely on Scheme 1 to interpret our kinetic data [9]. The rate constant for substrate association (k_{on}) is equivalent to k_{cat}/K_m. Transfer of the phosphate from pThr14 of the bis-phosphorylated substrate to form the phospho-enzyme intermediate and the mono-phosphorylated product is governed by k_2. Hydrolysis of the phospho-enzyme intermediate is governed by k_3 and is kinetically silent for both pNPP and protein substrate. In this kinetic scheme, $K_m = K_D/2$ for the substrate pNPP ($k_{off} \gg k_2$) and $K_m = k_2/2\ k_1$ for the protein substrate ($k_{-1} \gg k_2$) [16]. The temperature dependence of substrate binding was fitted with

$$R\ln\left(\frac{1}{K_m}\right) = -\frac{\Delta H}{T} + \Delta S \quad (1)$$

wherein R is the gas constant, ΔH is the enthalpy, T is the absolute temperature, and ΔS is the entropy. The temperature dependence of phosphate transfer and substrate association were fitted with

$$R\ln\left[k\left(\frac{h}{k_b T}\right)\right] = -\frac{\Delta H^{\ddagger}}{T} + \Delta S^{\ddagger} \quad (2)$$

wherein k is either derived from V_{max} in the K_m determinations for pNPP or the k_{on} derived from the k_{cat}/K_m for the protein substrate, k_b is Boltzmann's constant, h is Planck's constant, R is the gas constant, and T is the absolute temperature. These equations were fitted to the data using weighted least-square fitting in Excel (Microsoft). Errors were typically <20% for values of k_{cat}/K_m, k_{on}, or k_2 and are indicated in Tables 1 and 2.

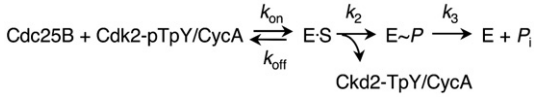

Scheme 1.

Table 1
Transition state activation parameters for phospho-transfer (all values in kcal/mol)

	$\Delta G^{\ddagger}$ at 298 K	$\Delta H^{\ddagger}$	$T\Delta S^{\ddagger}$ at 298 K
WT (pNPP)	18±4	20±4	2±1
WT (Cdk2-pTpY/CycA)	17±3	12±2	−6±2
R492L (Cdk2-pTpY/CycA)	20±3	16±2	−4±1

3. Results and discussion

3.1. The temperature dependence of Cdc25B with pNPP

We first studied the temperature dependence of Cdc25B phosphatase with the small molecule substrate *p*-nitrophenyl phosphate (pNPP) to focus on the simpler question of phosphate binding and formation of the phospho-cysteine intermediate within the active site alone. The substrate pNPP provides a particularly useful basis for comparison because of the similarities it shares with the kinetics of the protein substrate. Like Cdk2–pTpY/CycA, pNPP does not exhibit burst kinetics, with rate-limiting substrate association at low concentrations of substrate and rate-limiting formation of the phospho-cysteine intermediate at saturating concentrations of substrate [11]. For pNPP, the rate of chemistry is somewhat slower ($k_2 = 0.2$ vs. 1.2 s^{-1}), whereas the K_m is significantly higher (10 mM vs. 0.5 μM) compared to the protein substrate. The K_m for pNPP reflects to a large extent the binding affinity of inorganic phosphate at the active site ($K_d = 3$ mM [17]), suggesting that the rest of the molecule does not interact significantly with the active site. The K_m for pNPP also is presumably similar to the true K_d for pNPP given its low affinity and the slow rate of reaction (i.e. $k_2 \ll k_{off}$ in the definition of K_m for Scheme 1) [16].

Complete K_m determinations for pNPP were performed over a temperature range of 5–25 °C (Fig. 2). The thermodynamic parameters for substrate binding were obtained by fitting Eq. (1) to the data. The binding of pNPP, thus phosphate, at the active site is mostly driven by enthalpy (ΔH of binding = −6±1 kcal/mol) with a small favorable entropic contribution ($T\Delta S = 3\pm1$ kcal/mol at 298 K), presumably from the desolvation of phosphate and the active site. The overall negative ΔG (−8 kcal/mol at 298 K) suggests that phosphate binding at the

Table 2
Transition state activation parameters for protein substrate association (all values in kcal/mol)

	$\Delta G^{\ddagger}$ at 298 K	$\Delta H^{\ddagger}$	$T\Delta S^{\ddagger}$ at 298 K
Wild type	9±2	13±2	4±1
R488L	13±2	10±1	−3±1
R492L	12±2	15±2	3±1
Y497A	12±2	8±1	−4±1
D206A	12±2	16±2	3±1
Truncation	11±2	18±2	7±2

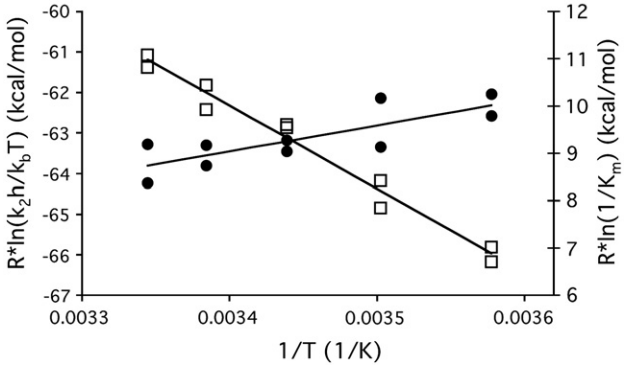

Fig. 2. Temperature dependence of K_m and k_2 for pNPP. The K_m (solid circle, right axis) and chemistry (open square, left axis) were determined over a range of temperatures (5–24 °C) for the substrate pNPP. Eqs. (1) and (2) were used to derive the thermodynamic parameters ΔH, $T\Delta S$, $\Delta H^{\ddagger}$, and $T\Delta S^{\ddagger}$. Data presented are mean values of at least three measurements and the experimental errors for each data point are ≤20%.

active site, albeit weak, is an overall thermodynamically favorable process.

We used transition state theory and the temperature dependence of the rate of phospho-cysteine formation with the substrate pNPP to shed further light on the kinetic and physical mechanism of Cdc25B [18]. The thermodynamic transition state activation parameters $\Delta H^{\ddagger}$ and $T\Delta S^{\ddagger}$ for the rate of chemistry (k_2) at standard conditions were determined with the Eyring plot using Eq. (2). The transition state activation energy for the formation of the phospho-cysteine intermediate with pNPP ($\Delta G^{\ddagger}=18$ kcal/mol at 298 K) is almost entirely determined by $\Delta H^{\ddagger}$ (20 kcal/mol), with a relatively small but favorable contribution of $T\Delta S^{\ddagger}$ (2 kcal/mol at 298 K; Fig. 2 and Table 1). Our thermodynamic analysis of the reaction with pNPP suggests that the active site of Cdc25B is pre-organized for effective phosphate binding and transfer to Cys473 with minimal if any conformational changes. This conclusion is consistent with existing structural data. First, the active site loop of Cdc25B can be superimposed on the active site loops of >20 other PTPs that share this same motif for which structures are known. Within the CX_5R motif of the active site loop, the backbone amides of the five X residues along with the conserved Arg coordinate the incoming phosphate perfectly for the catalytic cysteine thiolate to perform a nucleophilic attack to form the phospho-enzyme intermediate. More specifically for Cdc25B, the active site loop remains essentially identical in structures of sulfate-bound Cdc25B [19], apo-Cdc25B [20], and the active site mutant, C473S [7].

3.2. The temperature dependence of E.S formation for Cdc25B with protein substrate

We have previously demonstrated that the rate of association (k_{on}) for Cdc25B with its protein substrate is essentially identical to the steady state specificity constant (k_{cat}/K_m) (Scheme 1) [9]. Thus, we were able to readily investigate the temperature dependence of the association for Cdc25B with its protein substrate. We used the Eyring equation (Eq. (2)) to convert our data to the activation parameters for the transition state for E·S formation. For protein–protein association, the activation enthalpy includes primarily the energetic cost of breaking existing bonds (with water, buffer, and/or ion molecules) and forming new bonds (amino acid pairings) at the protein interface. The entropy is dictated by two factors. First, the loss of rotational and translational freedom of individual proteins, their interface residues in particular, is entropically unfavorable. Second, the release of solvent molecules from the newly forming interface is large and entropically favorable, easily compensating for the loss of internal entropy.

The overall transition state free energy barrier at standard state ($\Delta G^{\ddagger}$) for the association between Cdc25B and Cdk2–pTpY/CycA at 298 K is 9 kcal/mol with a $\Delta H^{\ddagger}$ of 13 kcal/mol and a favorable $T\Delta S^{\ddagger}$ of 4 kcal/mol (Fig. 3 and Table 2). The moderate magnitude of the activation enthalpy for Cdc25B association with protein substrate hints at the significant but not exclusive role of free diffusion in the association of protein substrate. A strictly diffusion controlled process is expected to have a low activation enthalpy of ~4 kcal/mol, whereas if the association is largely controlled by internal factors such as massive residue rearrangements, the $\Delta H^{\ddagger}$ tends to be greater than 20 kcal/mol [18]. The significant favorable entropic contribution of 4 kcal/mol is consistent with the desolvation that must occur during formation of the large protein–protein interface between Cdc25B and its protein substrate [7].

We next investigated the temperature dependence of E·S formation for the hotspot mutants (R488L, R492L, Y497A on

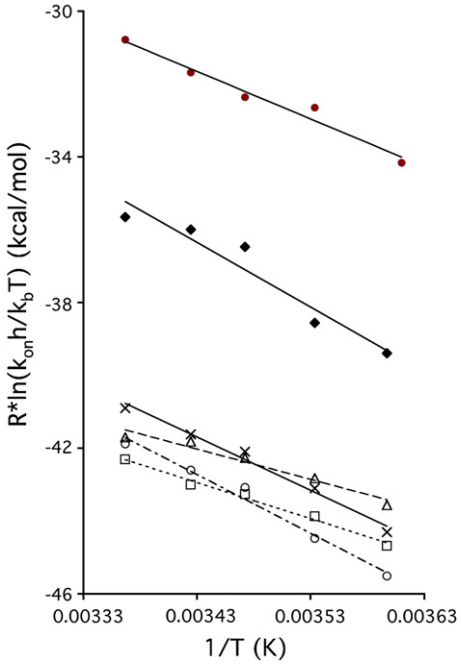

Fig. 3. The Eyring plot for the association of Cdc25 with protein substrate. The k_{cat}/K_m values reflecting the k_{on} values for wild type Cdc25B (closed circles), the C-terminal tail truncation (filled diamonds), R488L (open squares), Y497A (open triangles), R492L (crosses), mutants of Cdc25B and the D206A (open circles) mutant of protein substrate determined at 4–24 °C. Data shown are the mean values of at least three separate determinations. The error for the determined value at each temperature was ≤30% and the R^2 value for each linear fit was ≥0.92. The derived activation parameters are listed in Table 2.

Cdc25B and D206A on Cdk2) using k_{cat}/K_m measurements reflective of k_{on}. Although the thermodynamic transition state parameters for protein association reflect complex processes, we attempt here to interpret the enthalpy–entropy compensations for the different hotspot mutants [21–23]. The individual activation parameters $\Delta H^{\ddagger}$ and $T\Delta S^{\ddagger}$ were obtained using the Eyring plot (Fig. 3 and Table 2). As expected from our initial kinetic analysis, all the hotspot mutants had essentially identical $\Delta G^{\ddagger}$ values for association of protein substrate that are ~3 kcal/mol higher than for the wild type enzyme. However, the individual activation parameters for the hotspot mutants were markedly different from one another. The $\Delta H^{\ddagger}$ values for association of R488L and Y497A were significantly lower than for wild type Cdc25B, while the $T\Delta S^{\ddagger}$ terms became negative, reminiscent of the enthalpy–entropy compensations seen for binding of mutants in the Ras/Raf system wherein $\Delta\Delta H$ and $T\Delta\Delta S$ are consistently greater than $\Delta\Delta G$ [4]. Our data, however, are in stark contrast to the higher $\Delta H^{\ddagger}$ values seen for the blocking of favorable charge–charge interactions via mutagenesis or increasing salt concentrations in the Barnase/Barstar system [3]. We have previously established that the major contribution of Arg488 is to participate in an ionic network centered around Asp206 of the substrate [8], similar to the ionic network in Barnase/Barstar. The contrasting results in these two systems must therefore originate from other differences. First, the rate of association for Barnase/Barstar is truly diffusion-limited ($k_{on}=10^9$ M^{-1} s^{-1} [24], $\Delta H^{\ddagger}=4$ kcal/mol [3], strong viscosity dependence [24]), in contrast to Cdc25B/Cdk2–pTpY/CycA ($k_{on}=10^6$ M^{-1} s^{-1}, $\Delta H^{\ddagger}=13$ kcal/mol, no viscosity dependence [25]). Second, the effects of individual mutations for the Barnase/Barstar system on the rate of association are small compared to what we have observed for our hotspot mutants (~10-fold vs. ≥200-fold), with most mutations in Barnase/Barstar affecting the rates of dissociation. We conclude that the Arg488 and Tyr497 residues contribute to substrate association, not just through electrostatic steering, but rather by forming tight and specific interactions. That is, neither R488L nor Y497A can form as tight a complex with Cdk2–pTpY/CycA as wild type Cdc25B. These non-ideal interactions at the remote docking site thus lead to entropically unfavorable trapping of water at the interface.

Conversely, for R492L, $\Delta H^{\ddagger}$ was slightly higher compared to wild type enzyme, whereas the determined $T\Delta S^{\ddagger}$ was, although still positive, slightly less favorable than for wild type Cdc25B (Fig. 3 and Table 2). Coupled with our previous kinetic and structural data showing that R492L binds almost as tightly to protein substrate as wild type Cdc25B without any dramatic conformational changes [9], this tight yet unproductive formation of an E·S complex clearly requires more bond breakage and formation, thus displacing more bound water from the interface. This interpretation is consistent with the similar trend seen for the D206A mutant for which we have established the most significant energetic coupling with R492L (Fig. 3 and Table 2) [7,10].

We also investigated the temperature dependence of Cdc25B lacking the C-terminal tail (Fig. 3 and Table 2). We have previously shown that this tail, not visible in the crystal structure or in the docked model, is specifically involved in protein substrate recognition independent of the hotspot residues [7,10]. As for wild type Cdc25B and the hotspot mutants [9], we used single-turnover experiments to confirm that the steady state k_{cat}/K_m was reflective of the rate of association for the truncated mutant (data not shown). Interestingly, the transition state activation parameters of the truncated mutant were dramatically different from any of the hotspot mutants, with a significantly higher enthalpy yet a more favorable entropy than wild type. Thus, the C-terminal tail's contribution to substrate association, essentially equivalent to removal of two Arg residues (Arg556 and Arg562 in Cdc25B) [10], is more reminiscent of the electrostatic interactions seen in Barnase/Barstar [24–27]. That is, the role of this tail region is limited to electrostatics and is much simpler than for the hotspot residues. Also, the more favorable entropy of the truncated mutant compared to wild type Cdc25B suggests an ordering of this unstructured tail during formation of the interaction between Cdc25B and its protein substrate.

3.3. The temperature dependence of phosphate transfer for Cdc25B with protein substrate

We determined the thermodynamic parameters for phosphocysteine formation for wild type Cdc25B and the R492L mutant with the protein substrate using single-turnover methods to derive the rate constants (k_2) by fitting a first order exponential to the time-dependent appearance of inorganic phosphate (Fig. 4 and Table 1). For wild type Cdc25B, the overall Gibbs free energy barrier is 17 kcal/mol at 298 K with a $\Delta H^{\ddagger}$ of 12 kcal/mol and a $T\Delta S^{\ddagger}$ of −6 kcal/mol. The smaller $\Delta H^{\ddagger}$ in formation of the phospho-cysteine for protein substrate compared to pNPP may reflect the favorable contribution by the yet unidentified catalytic acid in protonation of the leaving group [11,28,29]. Alternatively, the hydrophobic environment afforded by the protein interface [7], which favors stabilization of a meta-phosphate-like transition state, may be responsible for this difference in $\Delta H^{\ddagger}$ values. In contrast to the small favorable

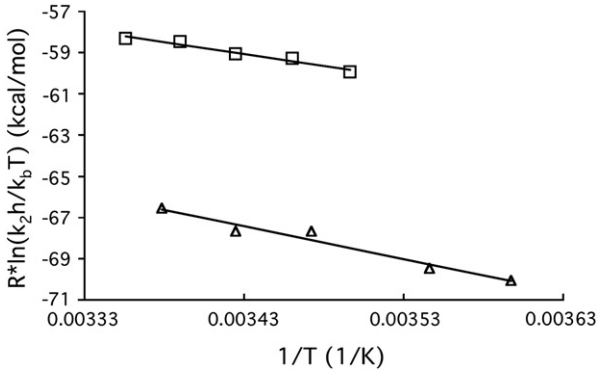

Fig. 4. The Eyring plot for phospho-transfer from Cdk2-pTpY/CycA to Cdc25B. The rates chemistry for wild type Cdc25B (open square) and the R492L mutant (open triangles) were determined over a range of temperatures (13–25 °C for wild type; 5–23 °C for R492L) for the substrate Cdk2-pTpY/CycA. Data presented are mean values of at least three measurements and the experimental errors for each data point are ≤20%.

entropic contribution seen in phospho-cysteine formation for pNPP, the negative contribution by $T\Delta S^{\ddagger}$ for the protein substrate is not negligible. Based on our results with pNPP, this unfavorable entropy is unlikely due to the reorganization of the active site loop itself. Rather, the unfavorable entropy more likely arises through formation of the tight solvent-excluded cavity at the active site upon binding of protein substrate [9]. The establishment of pair-wise interactions around the active site creating a suitable environment for phosphate transfer could account for this entropy loss and is consistent with promoting rapid dissociation of protein product, as we have observed experimentally [9]. Because our docked model of the E·S complex suggests that the target loop in Cdk2 containing pThr14 and pTyr15 must extend outward to reach the active site, it is also possible that the unfavorable entropy originates from the extension and immobilization of this loop [7]. Nevertheless, the dominant enthalpic term during formation of the phospho-enzyme using protein substrate does suggest that the k_{cat} of the reaction is determined more significantly by the breaking and forming of chemical bonds rather than reorganization of residues in the active site. Alternatively, enthalpically controlled enzymatic reactions have been explained using near attack conformations [30].

We next probed the thermodynamic basis for the large decrease in the rate of chemistry for the R492L mutant compared to wild type (0.016 vs. 1.2 s^{-1}) (Fig. 4 and Table 1). The $\Delta G^{\ddagger}$ of phosphate transfer by R492L was dominated by the $\Delta H^{\ddagger}$ term ($\Delta H^{\ddagger}=16$, $T\Delta S^{\ddagger}=-4$ kcal/mol at 298 K). The difference between wild type Cdc25B and the R492L mutant was most pronounced in $\Delta H^{\ddagger}$ (~4 kcal/mol). These data indicate that the physical basis for formation of the phospho-enzyme intermediate by the R492L mutant is still determined primarily by the energy required to break/form chemical bonds rather than by reorganization of active site residues. These results are consistent with the essentially identical crystal structures of R492L and wild type Cdc25B and our previous interpretation that the slowed rate of reaction is due to minor misalignment within the active site region [9].

4. Conclusion

As gleaned from numerous studies of tight stable protein complexes, specific and rapid protein association is generally thought to proceed via at least two steps, [31]. Diffusion and geometric constraints dictate the formation of an unstable encounter complex that subsequently progresses to a final docked complex. Formation of the largely still solvated encounter complex is driven in part by nonspecific hydrophobic interactions and specific long-range electrostatic interactions. Formation of the final docked complex is driven by desolvation and specific local hydrogen bonding. Our analysis of the much more transient interaction between the Cdc25B phosphatase and its protein substrate suggests that this two-step process is best described as a single concerted step. Kinetically, all determinations of rates of substrate association by either single-turnover experiments or by Biacore can be fitted to a first order exponential [9]. In conjunction with our double and triple mutant cycle analysis [8], our thermodynamic results presented herein point to the involvement of specific local interactions in the transition state for protein association. Whether this efficient yet transient mechanism for enzyme association with protein substrate extends to other systems remains to be determined.

Acknowledgement

This work was supported by NIH R01 GM61822.

References

[1] A.A. Bogan, K.S. Thorn, Anatomy of hot spots in protein interfaces, J. Mol. Biol. 280 (1) (1998) 1–9.
[2] T. Clackson, J.A. Wells, A hot spot of binding energy in a hormone–receptor interface, Science 267 (5196) (1995) 383–386.
[3] C. Frisch, A.R. Fersht, G. Schreiber, Experimental assignment of the structure of the transition state for the association of barnase and barstar, J. Mol. Biol. 308 (1) (2001) 69–77.
[4] C. Kiel, L. Serrano, C. Herrmann, A detailed thermodynamic analysis of Ras/Effector complex interfaces, J. Mol. Biol. 340 (2004) 1039–1058.
[5] W. Ito, H. Yasui, Y. Kurosawa, Mutations in the complementarity-determining regions do not cause differences in free energy during the process of formation of the activated complex between an antibody and the corresponding protein antigen, J. Mol. Biol. 248 (1995) 729–732.
[6] K.A. Xavier, R.C. Willson, Association and dissociation kinetics of anti-hen egg lysozyme monoclonal anitbodies HyHEL-5 and HyHEL-10, Biophys. J. 74 (1998) 2036–2045.
[7] J. Sohn, J.M. Parks, G. Buhrman, P. Brown, K. Kristjansdottir, A. Safi, H. Edelsbrunner, W. Yang, J. Rudolph, Experimental validation of the docking orientation of Cdc25 with its Cdk2/CycA protein substrate, Biochemistry 44 (2005) 16563–16573.
[8] J. Sohn, J. Rudolph, The energetic network of hotspot residues between Cdc25B phosphatase and its protein substrate, J. Mol. Biol. 362 (2006) 1060–1071.
[9] J. Sohn, G. Buhrman, J. Rudolph, in press. Kinetic and structural studies of specific protein–protein interactions in substrate catalysis by the Cdc25B phosphatase, Biochem.
[10] M. Wilborn, S. Free, A. Ban, J. Rudolph, The C-terminal tail of the dual-specificity Cdc25B phosphatase mediates modular substrate recognition, Biochemistry 40 (2001) 14200–14206.
[11] W. Chen, M. Wilborn, J. Rudolph, Dual-specific Cdc25B phosphatase: in search of the catalytic acid, Biochemistry 39 (35) (2000) 10781–10789.
[12] J. Sohn, K. Kristjánsdóttir, A. Safi, B. Parker, B. Kiburz, J. Rudolph, Remote hotspots mediate protein substrate recognition for the Cdc25 phosphatase, Proc. Natl. Acad. Sci. U. S. A. 47 (2004) 16437–16441.
[13] P.D. Jeffrey, A.A. Russo, K. Polyak, E. Gibbs, J. Hurwitz, J. Massagué, N.P. Pavletich, Mechanism of CDK activation revealed by the structure of a CyclinA–CDK2 complex, Nature 376 (1995) 313–320.
[14] K. Kristjánsdóttir, J. Rudolph, A fluorescence polarization assay for native protein substrates of kinases, Anal. Biochem. 316 (1) (2003) 41–49.
[15] J. Rudolph, D.M. Epstein, L. Parker, J. Eckstein, Specificity of natural and artificial substrates for human Cdc25A, Anal. Biochem. 289 (1) (2001) 43–51.
[16] I. Segel, Enzyme Kinetics, Wiley, New York, 1993.
[17] J. Sohn, J. Rudolph, Catalytic and chemical competence of regulation of Cdc25 phosphatase by oxidation/reduction, Biochemistry 42 (34) (2003) 10060–10070.
[18] H. Gutfreund, Kinetics for the Life Sciences, Cambridge University Press, Cambridge, 1995.
[19] R.A. Reynolds, A.W. Yem, C.L. Wolfe, M.R.J. Deibel, C.G. Chidester, K.D. Watenpaugh, Crystal structure of the catalytic subunit of Cdc25B required for G2/M phase transition of the cell cycle, J. Mol. Biol. 293 (1999) 559–568.
[20] G. Buhrman, B. Parker, J. Sohn, J. Rudolph, C. Mattos, Structural mechanism of oxidative regulation of the phosphatase Cdc25B via an intramolecular disulfide bond, Biochemistry 44 (2005) 5307–5316.

[21] E. Grunwald, C. Steel, Solvent reorganization and thermodynamic enthalpy–entropy compensation, J. Am. Chem. Soc. 117 (1995) 5687–5692.
[22] R. Lumry, Uses of enthalpy–entropy compensation in protein research, Biophys. J. 105 (2003) 545–557.
[23] R. Lumry, S. Rajender, Enthalpy–entropy compensation phenomena in water solutions of proteins and small molecules: a ubiquitous property of water, Biopolymers 9 (1970) 1125–1127.
[24] G. Schreiber, A.R. Fersht, Rapid, electrostatically assisted association of proteins, Nat. Struct. Biol. 3 (5) (1996) 427–431.
[25] T. Selzer, G. Schreiber, Predicting the rate enhancement of protein complex formation from the electrostatic energy of interaction, J. Mol. Biol. 287 (2) (1999) 409–419.
[26] T. Selzer, G. Schreiber, New insights into the mechanism of protein–protein association, Proteins 45 (3) (2001) 190–198.
[27] Y. Shaul, G. Schreiber, Exploring the charge space of protein–protein association: a proteomic study, Proteins 60 (2005) 341–352.
[28] J. Rudolph, Catalytic mechanism of Cdc25, Biochemistry 41 (2002) 14613–14623.
[29] J. Rudolph, Reactivity of Cdc25 phosphatase at low pH and with thiophosphorylated protein substrate, Bioorg. Chem. 33 (2005) 264–273.
[30] F.C. Lightstone, T.C. Bruice, Ground state conformations and entropic and enthalpic factors in the efficiency of intramolecular and enzymatic reactions: 1. Cyclic anhydride formation by substituted glutarates, succinate, and 3,6-endoxo-Δ4-tetrahydrophthalate monophenyl esters, J. Am. Chem. Soc. 118 (1996) 2595–2605.
[31] G. Schreiber, Kinetic studies of protein–protein interactions, Curr. Opin. Struct. Biol. 12 (2002) 41–47.